

**K-shell x-ray production in  $^{19}\text{K}$ ,  $^{22}\text{Ti}$ ,  $^{25}\text{Mn}$ , and  $^{35}\text{Br}$  by 20–80-MeV  $^{17}\text{Cl}^q$  ions**

J. A. Tanis

*Department of Physics and Astronomy, University of North Carolina, Chapel Hill, North Carolina 27514  
and Department of Physics, Western Michigan University, Kalamazoo, Michigan 49008\**S. M. Shafroth, W. W. Jacobs,<sup>†</sup> and T. McAbee*Department of Physics and Astronomy, University of North Carolina, Chapel Hill, North Carolina 27514  
and Triangle Universities Nuclear Laboratory, Durham, North Carolina 27607*

G. Lapicki

*Department of Physics, East Carolina University, Greenville, North Carolina 27834*

(Received 13 February 1984)

Target  $K$  x-ray production cross sections have been determined for 20–80-MeV  $^{17}\text{Cl}^q+$  ( $q=3-10$ ) ions incident on vanishingly thin ( $\sim 10 \mu\text{g}/\text{cm}^2$ ) targets of  $^{19}\text{K}$ ,  $^{22}\text{Ti}$ ,  $^{25}\text{Mn}$ , and  $^{35}\text{Br}$ . In addition, intensity ratios  $I_{K\beta}/I_{K\alpha}$  and  $K\alpha, K\beta$  x-ray energy shifts were measured. Using Hartree-Fock-Slater calculations and statistical scaling methods for multiple ionization, the number of  $2p$  and  $3p$  vacancies at x-ray emission is deduced from the  $K\alpha$  energy shifts and  $I_{K\beta}/I_{K\alpha}$ , respectively. From the number of  $2p$  and  $3p$  vacancies at x-ray emission the fluorescence yield  $\omega_K$  in the presence of this multiple ionization is then determined. The modified values of  $\omega_K$ , which are as much as 40% larger than the single-vacancy fluorescence yields, were used to compare the measured x-ray cross sections with theoretical predictions of ionization from the perturbed-stationary-state (PSS) theory with energy loss (E), Coulomb deflection (C), and relativistic (R) corrections, i.e., the ECPSSR theory of Brandt and Lapicki. Reasonable agreement with theory is obtained for  $^{17}\text{Cl} + ^{35}\text{Br}$  ( $Z_1/Z_2 \sim \frac{1}{2}$ ) with the agreement becoming progressively worse, as expected, for  $Z_1/Z_2 \rightarrow 1$ . The results provide evidence for the validity of the ECPSSR theory for collision systems with  $Z_1/Z_2 \simeq \frac{1}{2}$  even when  $v_1/v_{2K} \simeq 0.3$ .

**I. INTRODUCTION**

In the collision of a heavy ion with a thin solid target, an ion with a  $K$  vacancy produces a large enhancement in the measured  $K$  x-ray yields of both the projectile<sup>1</sup> and the target.<sup>2</sup> This enhancement is due to electron transfer from the target  $K$  shell to the projectile  $K$  shell. This  $K$ -to- $K$  electron transfer manifests itself by giving rise to x-ray yields which depend on target thickness due to the changing fraction of ions with  $K$  vacancies as the ions move through the foil. This target-thickness dependence of measured  $K$  x-ray yields has been observed in several experiments<sup>3-8</sup> and is found to occur for all incident charge states.

In order to obtain physically meaningful x-ray cross sections from such collisions, it is imperative that target-thickness effects be taken into account before comparing heavy-ion induced x-ray production cross sections with theoretical calculations. Specifically, to extract the single collision cross sections, the x-ray yields must be determined for vanishing thickness of the material in which they are produced. In the case of target x rays this can be done in a straightforward manner since target thicknesses as small as desired may be achieved by evaporating the target material onto a backing. If the target material of interest is positioned to face the incident beam, then the backing material will have no effect on the measured tar-

get x-ray yields. In the case of projectile x-ray yields, self-supporting foils must be used and the measured yield must be extrapolated to vanishing target thickness. We have previously reported<sup>8</sup> measurements of both target and projectile  $K$  x-ray production as a function of target thickness for 20–80-MeV  $\text{Cl}$  ions incident on self-supporting  $\text{Cu}$  targets.

In this work we report measurements of *target*  $K$  x-ray yields for 20–80-MeV  $\text{Cl}^q+$  ( $q=3-10$ ) incident on vanishingly thin targets of  $\text{K}$ ,  $\text{Ti}$ ,  $\text{Mn}$ , and  $\text{Br}$ . Projectile x-ray yields were not obtained due to the difficulty in making self-supporting foils for these target species. The measured x-ray cross sections, after their conversion with fluorescence yields modified for multiple ionization, are compared with theoretical predictions of ionization.<sup>9-12</sup>

**II. EXPERIMENTAL PROCEDURE**

The experimental setup used in this work has been described in detail previously<sup>8</sup> and hence only a brief outline will be given here. Chlorine ions obtained from the Triangle Universities Nuclear Laboratory FN tandem Van de Graaff were incident on thin targets of  $\text{KBr}$ ,  $\text{Ti}$ , and  $\text{Mn}$ . (The  $\text{K}$  and  $\text{Br}$  data were collected simultaneously.) X rays were detected in air at  $90^\circ$  to the beam with a  $\text{Si}(\text{Li})$  detector having a  $25.4\text{-}\mu\text{m}$   $\text{Be}$  window. The detector viewed the target through a  $25.4\text{-}\mu\text{m}$  Mylar window

and, in addition, a 12.7- $\mu\text{m}$  aluminum absorber was used to attenuate the x rays in order to minimize pileup and dead-time effects. Counting rates were generally  $\leq 400/\text{s}$ . Absolute normalization of the incident-beam intensity was accomplished by detecting elastically scattered Cl ions in a silicon surface barrier detector mounted at  $60^\circ$  to the incident-beam direction.

The targets were prepared by vacuum evaporation onto  $\sim 20\text{-}\mu\text{g}/\text{cm}^2$  carbon backings. Absolute target thicknesses were determined to about  $\pm 5\%$  by measuring the Coulomb-scattered chlorine ions emerging from the target. This of course requires knowledge of the average equilibrium charge of the ions emerging from the target. The thicknesses of the targets so obtained are given in Table I. As a check on the thicknesses so determined, Rutherford scattering by 10-MeV oxygen ions and 3-MeV protons were used in some cases. Absolute values of the thicknesses obtained with all three ions generally agreed to better than 10%.

Sufficient counting statistics were obtained for each x-ray and particle yield so that statistical errors were  $\leq 3\%$ . Measured x-ray yields were corrected for detector efficiency which was calculated from tabulated photon-absorption cross sections<sup>13</sup> for the various absorbers.

### III. RESULTS

X-ray production cross sections deduced from the present measurements are listed in Table II. All cross sections were generally reproducible to better than  $\pm 10\%$ , while the absolute uncertainties due to all sources (including nonzero target thickness) are estimated to be  $+40\%$  and  $-20\%$ . Also shown in the table are previous results<sup>8</sup> obtained for copper. All data were obtained using ions with incident charge states  $q < Z_1 - 2$  ( $=15$ ). Use of these charge states minimizes the possibility of target K-electron transfer to the projectile K shell (except for a small contribution due to finite target thickness). Thus, very little of the target K x-ray yield is due to this K-to-K transfer. Such enhancement is known to be large.<sup>2-8</sup> For projectiles incident with a full K shell, target K x-ray production has been shown<sup>2</sup> to be nearly insensitive to the precise charge state of the projectile.

In Fig. 1 we show the intensity ratios  $I_{K\beta}/I_{K\alpha}$  for each of the targets. For  $^{19}\text{K}$  this ratio could not be reliably obtained for energies less than 50 MeV due to overlap of the projectile radiative electron-capture (REC) peak with the potassium K x rays. Likewise, overlap of the REC with

TABLE I. Thicknesses of the targets used in this work. Values were obtained from the Coulomb-scattered chlorine ions emerging from the target.

Target	Thickness ( $\mu\text{g}/\text{cm}^2$ )	Thickness ( $10^{16}$ atoms/ $\text{cm}^2$ )
$^{19}\text{K}^a$	$7.6 \pm 0.4$	$11.7 \pm 0.6$
$^{22}\text{Ti}$	$3.9 \pm 0.2$	$4.8 \pm 0.2$
$^{25}\text{Mn}$	$7.3 \pm 0.4$	$8.0 \pm 0.4$
$^{35}\text{Br}^a$	$15.5 \pm 0.8$	$11.7 \pm 0.6$

<sup>a</sup>KBr used for this target.

TABLE II. Target K x-ray production cross sections resulting from  $^{17}\text{Cl}^{9+}$  ion bombardment. The copper data are from Ref. 8. All cross sections were measured for vanishingly thin targets (see Table I). Relative uncertainties are  $\pm 10\%$ ; absolute uncertainties are estimated to be between  $+40\%$  and  $-20\%$  except for  $^{29}\text{Cu}$  for which the absolute uncertainty is  $\pm 20\%$ . The larger positive uncertainty ( $+40\%$ ) results from the error due to nonzero target thickness for K, Ti, Mn, and Br.

E (MeV)	Charge state q	Cross section (b)				
		$^{19}\text{K}$	$^{22}\text{Ti}$	$^{25}\text{Mn}$	$^{29}\text{Cu}^a$	$^{35}\text{Br}$
20	3	10 800	1590	205	7.0	
30	6	26 100	4800	938		
40	7	44 600	11 700	2930	190	20.1
50	7	57 300	14 700	5340		56.5
60	8	103 000	32 500	10 100	1100	145
80	10	164 000			3500	419

<sup>a</sup>From Ref. 8.

the Ti K x rays prevented the  $^{22}\text{Ti}$   $I_{K\beta}/I_{K\alpha}$  from being accurately determined for energies greater than 60 MeV. Qualitatively, the increasing  $I_{K\beta}/I_{K\alpha}$  ratio indicates that the degree of 3p subshell ionization relative to 2p subshell ionization at the time of x-ray emission decreases with beam energy. On the right side of the figure are shown the  $I_{K\beta}/I_{K\alpha}$  ratios calculated by Scofield<sup>14</sup> for ions having only a single vacancy.

In addition to the K x-ray cross sections and the  $I_{K\beta}/I_{K\alpha}$  ratios, we determined the average  $K\alpha$  and  $K\beta$  x-ray energy shifts for each target at x-ray emission. These results are shown in Fig. 2 ( $K\beta$  x-ray shifts were not obtained for Br.) The increase in both the  $K\alpha$  and  $K\beta$  energy shifts indicate that the L-shell ionization increases with increasing beam energy. The  $I_{K\beta}/I_{K\alpha}$  ratios and the x-ray energy shifts can be used to estimate the degree of 2p and 3p ionization at the time of x-ray emission as discussed in the next section.

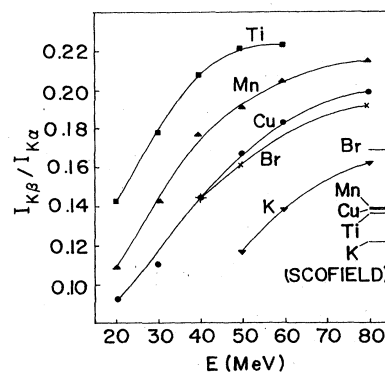


FIG. 1. Target intensity ratios  $I_{K\beta}/I_{K\alpha}$  for 20–80-MeV Cl + K, Ti, Mn, Cu, and Br. Uncertainties in these values are about the size of the data points. Measurements of  $I_{K\beta}/I_{K\alpha}$  were not obtained for  $^{19}\text{K}$  for  $E < 50$  MeV and for  $^{22}\text{Ti}$  for  $E > 60$  MeV due to overlap of the radiative electron capture (REC) with the characteristic x-rays. Lines are drawn to guide the eye. The  $I_{K\beta}/I_{K\alpha}$  ratios labeled Scofield on the right side of the figure are from Ref. 14 and are the theoretical  $I_{K\beta}/I_{K\alpha}$  ratios for a single vacancy.

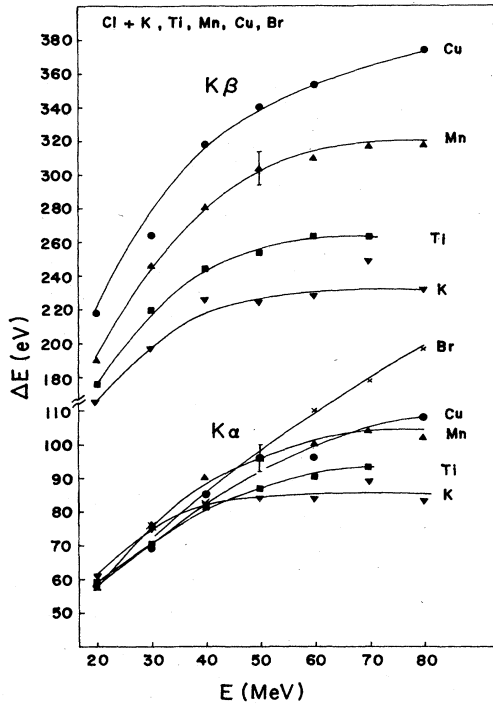


FIG. 2. Target  $K\alpha$  and  $K\beta$  x-ray energy shifts for 20–80-MeV Cl ions.  $K\beta$  shifts were not obtained for Br. Lines are drawn to guide the eye.

#### IV. DISCUSSION

##### A. Fluorescence yields for multiply ionized atoms

As mentioned above, the shifts in the measured  $K\alpha$  and  $K\beta$  x-ray energies are due primarily to multiple  $L$ -shell vacancies at  $K$  x-ray emission, while the variation in  $I_{K\beta}/I_{K\alpha}$  reflects changes in the relative amount of  $2p$  and  $3p$  subshell ionization simultaneous with  $K$  x-ray emission.

These changes in  $2p$  and  $3p$  subshell ionization can be quantified. Since the shift in the  $K\alpha$  and  $K\beta$  x-ray energies are primarily due to  $L$ -shell vacancies, Hartree-Fock-Slater<sup>15</sup> (HFS) calculations can be used to correlate the number of  $2p$  vacancies with a given energy shift. The results of these calculations for both  $K\alpha$  and  $K\beta$  x rays are

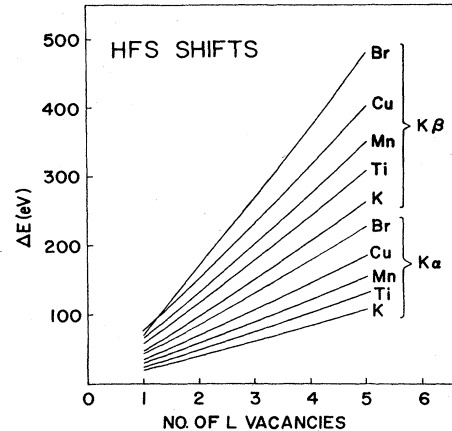


FIG. 3. Theoretical  $K\alpha$  and  $K\beta$  x-ray energy shifts as a function of  $2p$  vacancies obtained from Hartree-Fock-Slater calculations (Ref. 15).

shown in Fig. 3. It should be noted that even though  $K\beta$  involves a transition from the  $M$  shell, the shift in this  $K$  x-ray energy is due mostly to  $L$  vacancies since the shifts due to  $M$  vacancies are generally about an order-of-magnitude smaller than those due to  $L$  vacancies.

From Figs. 2 and 3 the average number of  $2p$  vacancies,  $V_{2p}$ , at x-ray emission can be determined for each beam energy. The results are shown in Table III for both  $K\alpha$  and  $K\beta$  x rays. One notes that the average number of  $2p$  vacancies determined from the  $K\beta$  x-ray energies is generally higher than that determined from the  $K\alpha$  x-ray energies. Qualitatively, this result might be expected since the presence of more  $2p$  vacancies would enhance  $K\beta$  relative to  $K\alpha$ . This is consistent with the fact that the  $I_{K\beta}/I_{K\alpha}$  ratio is enhanced over that for a single  $K$  vacancy.

By knowing the average number of  $2p$  vacancies at x-ray emission, the average number of  $3p$  vacancies,  $V_{3p}$ , can be estimated from the measured  $I_{K\beta}/I_{K\alpha}$ . Using the statistical scaling procedure of Larkins,<sup>16</sup>  $I_{K\beta}/I_{K\alpha}$  in the presence of  $2p$  and  $3p$  vacancies is given by

$$\frac{I_{K\beta}}{I_{K\alpha}} = \frac{I_{K\beta}^0}{I_{K\alpha}^0} \left( \frac{n_{3p}/6}{n_{2p}/6} \right) = \frac{I_{K\beta}^0}{I_{K\alpha}^0} \left( \frac{1 - \frac{V_{3p}}{6}}{1 - \frac{V_{2p}}{6}} \right), \quad (1)$$

TABLE III. Average number of  $2p$  vacancies,  $V_{2p}$ , present at x-ray emission for  $K\alpha$  and  $K\beta$  rays. These values were determined from Hartree-Fock-Slater calculations (Ref. 15) using Figs. 2 and 3.

$E$ (MeV)	Number of $2p$ vacancies									
	K		Ti		Mn		Cu		Br	
	$K\alpha$	$K\beta$	$K\alpha$	$K\beta$	$K\alpha$	$K\beta$	$K\alpha$	$K\beta$	$K\alpha$	$K\beta$
20	3	3.3	2.5	2.9	2.0	2.8	1.7	2.8		
30	3.8	3.8	2.9	3.7	2.6	3.6	2.0	3.5	1.7	
40	4	4.3	3.3	4.0	3.1	4.1	2.4	4.0	2.0	
50	4.2	4.3	3.5	4.2	3.3	4.4	2.7	4.3	2.3	
60	4.2	4.4	3.6	4.3	3.5	4.5	2.9	4.5	2.5	
70	4.2	4.4	3.7	4.3	3.6	4.6	3.0	4.6	2.7	
80	4.2	4.4			3.6	4.6	3.1	4.7	2.9	

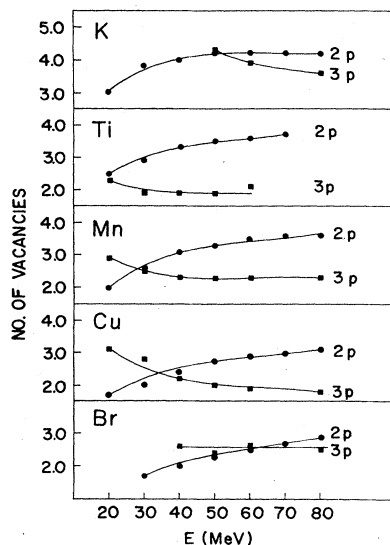


FIG. 4. Calculated number of  $2p$  and  $3p$  vacancies at x-ray emission as a function of beam energy. Number of  $2p$  vacancies (see Table III) was obtained from  $K\alpha$  energy shifts using Figs. 2 and 3. The number of  $3p$  vacancies was calculated from Eq. (1).

where  $n_{2p}$  and  $n_{3p}$  are the number of  $2p$  and  $3p$  electrons present at x-ray emission and  $I_{K\beta}^0/I_{K\alpha}^0$  is the ratio for an atom having only a single vacancy. Using the value of  $I_{K\beta}^0/I_{K\alpha}^0$  from Scofield,<sup>14</sup> the values of  $V_{2p}$  from Table III for  $K\alpha$  and the value of  $I_{K\beta}/I_{K\alpha}$  from Fig. 1, the average number of  $3p$  vacancies  $V_{3p}$  can be calculated. (Note that  $V_{2p} = 6 - n_{2p}$  and  $V_{3p} = 6 - n_{3p}$ .)

The results of this calculation are shown in Fig. 4. Also shown in the figure is the number of  $2p$  vacancies  $V_{2p}$  associated with  $K\alpha$  as listed in Table III. It is seen that  $V_{2p}$  increases over the energy range investigated while  $V_{3p}$  slowly decreases. These variations in  $V_{2p}$  and  $V_{3p}$  are qualitatively consistent with the measured trends in the  $K\alpha$  and  $K\beta$  energy shifts and the  $I_{K\beta}/I_{K\alpha}$  ratios.

The variation in  $V_{2p}$  and  $V_{3p}$  with beam energy can then be used to calculate the change in the fluorescence yield  $\omega_K$  for each target (due to multiple  $2p$  and  $3p$  sub-shell ionization) using the statistical scaling procedure of Larkins.<sup>16</sup> This calculation is described in the Appendix.

Table IV shows the modified values of  $\omega_K$  obtained from the statistical scaling. The modified  $\omega_K$  exhibit little beam-energy dependence ( $< 8\%$  in all cases) and so the average value of  $\omega_K$  was used for each target. These values of  $\omega_K$  will be used below to convert the measured x-ray production cross sections to ionization cross sections.

### B. Target ionization cross sections

Experimental  $K$ -shell ionization cross sections are obtained after division of the  $K$ -x-ray production cross sections of Table II by the fluorescence yields of Table IV. These cross sections are plotted in Figs. 5–9.

These measured ionization cross sections are compared with the predictions (solid curves) of the ECPSSR theory<sup>9,10</sup> which accounts for the effects of the projectile energy loss ( $E$ ) and Coulomb deflection ( $C$ ) and goes beyond the unperturbed and nonrelativistic treatment of the  $K$ -shell electron in perturbed-stationary-state (PSS) and relativistic (R) ways. The ECPSSR curves represent ionization cross sections calculated as the cross-section sum of electron capture to unoccupied bound states of the projectile<sup>9</sup> and of direct ionization to the target continuum.<sup>10</sup> The states into which the target  $K$ -shell electron can be captured are defined by the charge states of chlorine ions that, in targets of nearly zero thickness (see Table I), are taken as the incident charge states  $q$  of the bombarding  $\text{Cl}^{q+}$  beam (see Table II). With capture to the  $K$  shell of such projectiles being impossible and with the transfer to the  $L$  shell allowed only partially at the highest available charge states of  $q \geq 8$ , electron capture<sup>9</sup> contributes to the total ionization<sup>9,10</sup> merely  $\sim 1$ – $23\%$  for all collision systems in our study. As expected, this contribution decreases with increasing  $Z_2$ ; it is in the  $14$ – $23\%$  range for  $^{19}\text{K}$  and barely  $1$ – $4\%$  of the total ionization in  $^{35}\text{Br}$ . In this sense, our ionization data test primarily direct ionization theories.

To illustrate how the ECPSSR approach differs from the first Born approximation, we show (dashed curves in Figs. 5–9) the sum of the cross sections calculated in the plane-wave Born approximation (PWBA) for direct ionization<sup>11</sup> and the Oppenheimer-Brinkman-Kramers (OBK) treatment of Nikolaev<sup>12</sup> for electron capture. While the

TABLE IV. Fluorescence yields modified for multiple ionization according to Eq. (A5a). Vacancy numbers  $V_{2p}$  and  $V_{3p}$  were obtained from Fig. 4. For each target a single arithmetic average  $\bar{\omega}_K$  was obtained since  $\omega_K/\omega_K^0$  is nearly independent ( $< 8\%$  variation) of the projectile energy.

Target	$\omega_K^0$ <sup>a</sup>	$\frac{\Gamma_{K\beta}^0}{\Gamma_{K\alpha}^0}$ <sup>b</sup>	$\frac{\Gamma_{KLL}^0}{\Gamma_A^0}$ <sup>c</sup>	$\frac{\Gamma_{KLM}^0}{\Gamma_A^0}$ <sup>c</sup>	$\frac{\omega_K}{\omega_K^0}$	$\bar{\omega}_K$
$^{19}\text{K}$	0.140	0.116	0.75	0.25	1.40	0.20
$^{22}\text{Ti}$	0.214	0.130	0.72	0.28	1.26	0.27
$^{25}\text{Mn}$	0.308	0.134	0.72	0.28	1.22	0.38
$^{29}\text{Cu}$	0.440	0.134	0.72	0.28	1.14	0.50
$^{35}\text{Br}$	0.618	0.152	0.69	0.31	1.10	0.68

<sup>a</sup>Ref. 26.

<sup>b</sup>Ref. 14.

<sup>c</sup>Ref. 27.

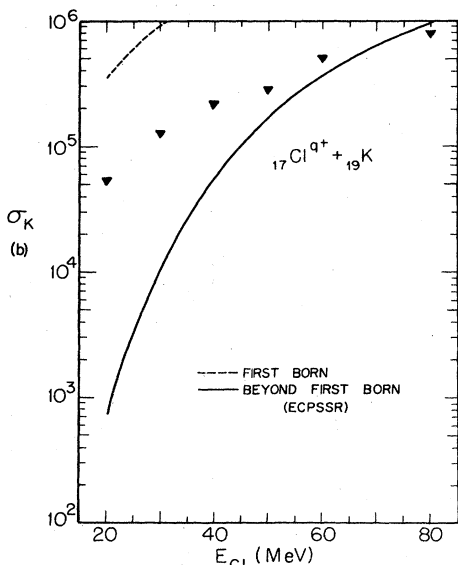


FIG. 5. Target  $K$ -shell ionization cross sections for Cl + K collisions. The dashed curve represents the first Born approximation of Refs. 11 and 12. The solid curve is based on Refs. 9 and 10.

first Born approximation overestimates the data by an order of magnitude, the ECPSSR theory converges to experiment as  $Z_1/Z_2$  decreases from 0.89 to 0.49 (going from Fig. 5 to Fig. 9). For  $^{17}\text{Cl} + ^{19}\text{K}$  (see Fig. 5), the first Born approximation overestimates the data to an equally disastrous extent as the predictions of ECPSSR theory underestimate these experimental points.

Since direct ionization, as argued before, is the main contributor to ionization (as opposed to electron capture) in the collision systems of our investigations, we conclude

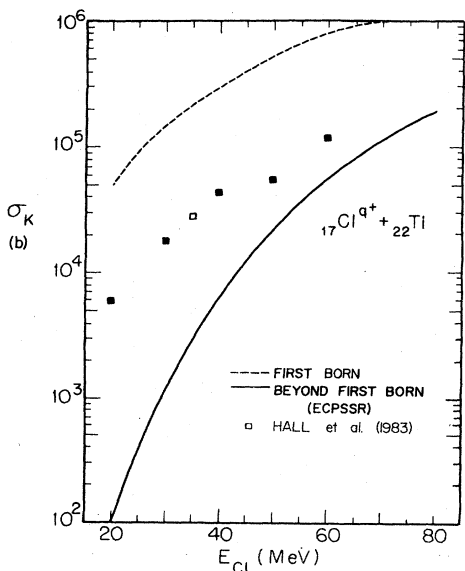


FIG. 6. Target  $K$ -shell ionization cross sections for Cl + Ti collisions. See caption for Fig. 5. The point at 35 MeV (open square) is from Ref. 17 and has been multiplied by 0.25/0.27 to correct for our estimate of  $\bar{\omega}_K$  vs the  $\bar{\omega}_K$  of Ref. 17.

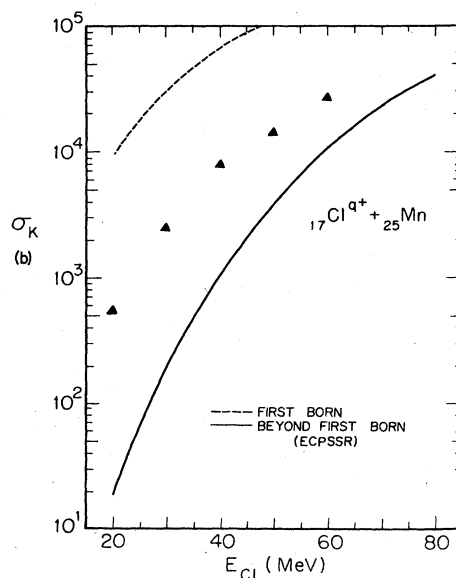


FIG. 7. Target  $K$ -shell ionization cross sections for Cl + Mn collisions. See caption for Fig. 5.

that the results of the direct ionization theory of Ref. 10 fall *below* the experimental points as  $Z_1/Z_2 \rightarrow 1$ . As analyses<sup>6,9</sup> of available data taken with fully stripped projectiles—for which electron capture is an overwhelming contributor to ionization at large  $Z_1/Z_2$ —indicate, the electron capture theory of Ref. 9 tends to lie *above* the experiment when  $Z_1/Z_2 \rightarrow 1$ .

These observations signal a possibility of the fortuitous agreement between the ionization theory based on Refs. 9 and 10 and future experiments in which  $Z_1/Z_2$  will ap-

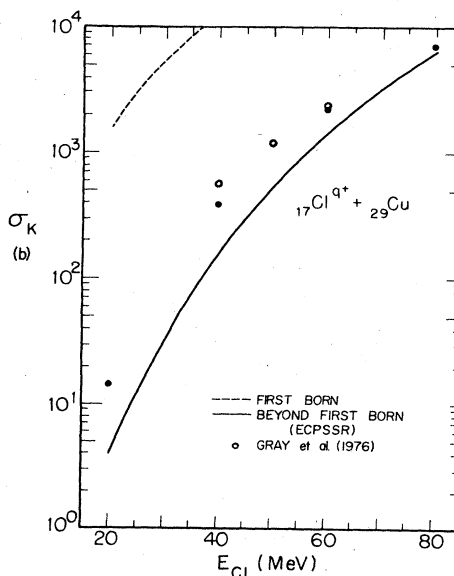


FIG. 8. Target  $K$ -shell ionization cross sections for Cl + Cu collisions. See caption for Fig. 5. Open circles are the  $\sigma_{KX}$  from Fig. 2 of Ref. 2 (at zero target thickness) and are divided by  $\bar{\omega}_K = 0.5$  from Table IV of the present work.

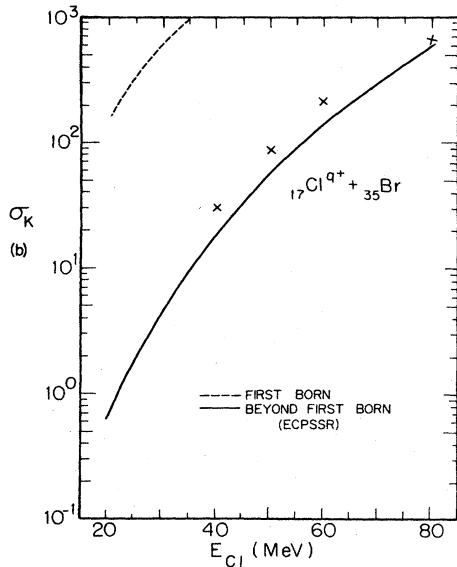


FIG. 9. Target  $K$ -shell ionization cross sections for  $\text{Cl} + \text{Br}$  collisions. See caption for Fig. 5.

proach unity and  $1 \ll q \ll Z_1$ . Electron capture and direct ionization may then contribute equally to ionization; inadequacies, inherent to the perturbative treatment<sup>9,10</sup> of such a system, will be buried in ionization studies as large but opposite deviations from the data in the calculations of electron capture<sup>9</sup> and direct ionization<sup>10</sup> will offset each other.

It cannot be construed from the preceding paragraph, however, that the ionization cross sections calculated according to Refs. 9 and 10 show only *accidentally* good agreement with the data when  $Z_1/Z_2 \leq \frac{1}{2}$ . In such systems it has been asserted and proven that a good agreement exists for total ionization as well as for electron capture.<sup>6,9</sup> A 10% agreement of the ionization data with the theory for  $Z_1/Z_2 \ll 1$  gives credence to the validity of the ECPSSR treatment of direct ionization.<sup>10</sup> Fair agreement of this theory with the  $_{17}\text{Cl}^{q+}$  ( $q=7,8,10$ ) on  $_{35}\text{Br}$  ( $Z_1/Z_2=0.49$ ) data reported in this work, in conjunction with insignificant contributions of electron capture for  $q \leq 10$ , seem to extend the range of its validity to all  $Z_1/Z_2 \leq \frac{1}{2}$ . Thus we conclude that the agreement in total ionization between the calculations of Refs. 9 and 10 and the data for such collision systems cannot be viewed as fortuitous.

Recently Hall *et al.*<sup>17</sup> reported  $K$ -shell x-ray production cross sections in titanium. With wide ranges of projectile atomic number and velocity, these data cover our ranges of  $Z_1/Z_2$  and  $v_1/v_{2K}$  and extend them down to 0.27 in  $Z_1/Z_2$  and up to 0.85 in  $v_1/v_{2K}$ . The 1-MeV/amu (35 MeV)  $_{17}\text{Cl} + _{22}\text{Ti}$  cross section of Ref. 17 is in excellent agreement with our data as shown in Fig. 6. It should be noted, however, that the incident chlorine charge state (not given) in Ref. 17 may be different from that of the present work. Since Hall *et al.* assume that electron capture occurs into a fully vacant  $L$  shell of chlorine, we infer that the 1-MeV/amu  $\text{Cl}$  was in the  $q=15$  charge state. In our experiments a 1-MeV/amu  $\text{Cl}$

ion would be at most in the  $q=7$  charge state, i.e., the electron could be captured only into  $M, N, \dots$  shells on the projectile. We calculate, in the ECPSSR theory,<sup>9,10</sup> that electron capture would contribute about 7% to the total ionization as contrasted with a 30% contribution when the  $\text{Cl } L$  shell is presumed to be empty; if the  $L$  shell were one-half filled, then the electron-capture contribution would be  $\sim 20\%$ . Since the data for  $q=7$  and  $q=15$  are in near agreement, we conclude that the electron-capture contribution is, in fact, small.

Also, in Ref. 17 the ECPSSR theory for electron capture<sup>9</sup> is dismissed as not *ab initio* calculations<sup>18</sup> and yet for direct ionization these authors rely on Ref. 19, an early version of the ECPSSR theory.<sup>10</sup> We have to note again<sup>9,20</sup> the error in theoretical interpretation that Ref. 17 makes in a manner similar to that previously done in Refs. 7 and 21. The authors simply scale the OBK cross sections of Nikolaev<sup>12</sup> by a purely empirical factor "to facilitate comparison with measured cross sections"<sup>17</sup> and they proceed to make a judgment on the validity of Ref. 19 as a function of  $Z_1/Z_2$  and  $v_1/v_{2K}$ . Could it not be that the validity of the chosen scaling factor might be in question? Unless the *scaled* electron-capture cross sections are very small by comparison with the direct ionization cross sections, there is no basis to assess *any* direct ionization theory to within a factor of 2. In Refs. 7, 17, and 21 the scaled cross sections are often forced to be as much as an order-of-magnitude larger than the direct ionization calculations. From the total ionization cross sections, measured with uncertainties that are larger than the predicted direct ionization cross sections, serious pronouncements are made on the direct ionization theory in Refs. 7, 17, and 21.

Finally, in Fig. 10 we show the region in which the data

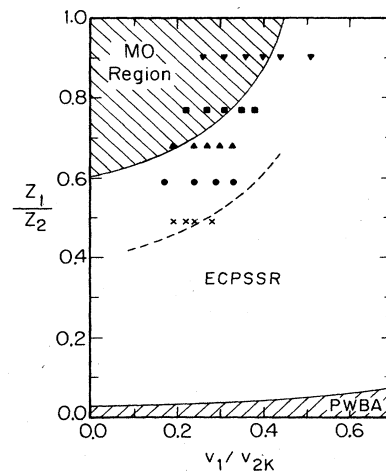


FIG. 10. Plot showing the region where the data of the present experiment were taken in comparison with the regions where the MO model and PWBA are expected to be valid (see text).  $Z_1$  and  $Z_2$  are projectile and target atomic numbers, respectively.  $v_1$  and  $v_{2K}$  are the projectile velocity and mean target  $K$ -electron velocity, respectively. The region below the dashed curve is where the ECPSSR theory (Refs. 9 and 10) is considered to be applicable. Symbols represent particular collision systems as follows: ( $\nabla$ )  $_{17}\text{Cl} + _{19}\text{K}$ , ( $\blacksquare$ )  $_{17}\text{Cl} + _{22}\text{Ti}$ , ( $\blacktriangle$ )  $_{17}\text{Cl} + _{25}\text{Mn}$ , ( $\bullet$ )  $_{17}\text{Cl} + _{29}\text{Cu}$ , ( $\times$ )  $_{17}\text{Cl} + _{35}\text{Br}$ .

of the present experiment were taken in comparison with the regions where the molecular-orbital (MO) model and the PWBA are generally expected to be valid. This figure is patterned after one by Madison and Merzbacher.<sup>22</sup> The lower shaded area is the region where the PWBA theory<sup>11</sup> is applicable. The upper shaded area (drawn somewhat arbitrarily<sup>23</sup>) is the region where the MO model should be valid. The region below the dashed curve is where the ECPSSR theory<sup>9,10</sup> is generally considered to be applicable.

It is seen that the present data fall nearer the MO region. The Cl + K data are seen to lie almost entirely in the MO region while the Cl + Ti data also fall partially in this region. Only for Cl + Br are the data close to the region where the ECPSSR is believed to be valid. Figure 10 is in substantial agreement with the results of Figs. 5–9 in which the present data are compared to the ECPSSR theory. In Figs. 5–9 only the Cl + Br data and possibly the Cl + Cu data are reasonably well represented by the ECPSSR theory. For the other data a molecular-orbital calculation is required. In the region of slow ( $v_1/v_{2K} \ll 1$ ) and near-symmetric ( $Z_1 \sim Z_2$ ) collisions, the MO model has been very recently reconciled<sup>24</sup> with the atomic description that is anchored on the united atom model of Briggs.<sup>25</sup> A perturbative or a coupled-state extension of the MO region in Fig. 10 toward the dashed boundary of the ECPSSR domain is still needed. Analyses of the collision systems, which fall in the gap between the regions of validity of MO and ECPSSR atomic theories, become unclear once direct ionization, electron capture, and molecular-orbital promotion vie in a competitive manner for the same  $K$ -shell electron. In particular, the  $2p\sigma$ - $2p\pi$  rotational coupling might enhance electron capture by opening additional channels for transfer to the  $L$  shell.

## V. CONCLUSION

Target  $K$  x-ray production by 20–80-MeV Cl ions incident on thin targets of K, Ti, Mn, and Br has been measured. Cross sections for  $K$ -shell ionization have been compared with the ECPSSR theory of Brandt and Lapicki<sup>9,10</sup> after modifying the target fluorescence yields to account for the presence of multiple  $2p$  and  $3p$  vacancies at x-ray emission. The numbers of  $2p$  and  $3p$  vacancies were deduced from measurements of the target intensity ratios  $I_{K\beta}/I_{K\alpha}$  and the  $K\alpha$  and  $K\beta$  x-ray energy shifts. Reasonable agreement of the measured cross sections with theory is obtained for Cl + Br ( $Z_1/Z_2 \sim \frac{1}{2}$ ) with the agreement becoming progressively worse for  $Z_1/Z_2 \rightarrow 1$ , as expected. The present results provide evidence for the validity of the ECPSSR theory for collision systems with  $Z_1/Z_2 \sim \frac{1}{2}$  even when  $v_1/v_{2K} \approx 0.3$ .

## ACKNOWLEDGMENTS

This work was supported in part by the U.S. Department of Energy, Division of Chemical Sciences. One of us (J.A.T.) was also supported in part by a grant from the North Carolina Board of Science and Technology.

## APPENDIX

In order to compare experimental x-ray production cross sections with theoretical ionization cross sections it is necessary to know the fluorescence yield  $\omega_K$  since  $\sigma_{KX} = \omega_K \sigma_K$ . Although the values of  $\omega_K$  are well-known<sup>26</sup> in the case where there is only a single vacancy and no other vacancies present,  $\omega_K$  is not well-known when there are multiple vacancies present at x-ray emission. When the single-vacancy fluorescence yield is in the region of  $\sim 0.10$ , multiple  $2p$  and  $3p$  vacancies may increase  $\omega_K$  by as much as a factor of 40% or more. Hence, it is important to account for these changes in  $\omega_K$  when comparing measured x-ray cross sections with ionization theories.

Changes in  $\omega_K$  due to the presence of multiple  $2p$  and  $3p$  vacancies can be calculated using the statistical scaling procedure of Larkins.<sup>16</sup> According to this technique, x-ray and Auger transition rates are assumed to scale in proportion to the number of electrons available to make the transition.

The fluorescence yield  $\omega_K$  is given by

$$\omega_K = \frac{\Gamma_X}{\Gamma_X + \Gamma_A}, \quad (\text{A1})$$

where  $\Gamma_X$  and  $\Gamma_A$  are the x-ray and Auger transition rates, respectively. Then

$$\omega_K^0 \Gamma_A^0 = (1 - \omega_K^0) \Gamma_X^0, \quad (\text{A2})$$

where the superscript indicates the rates for a single vacancy only. Using the statistical scaling technique,<sup>16</sup> the relevant transition rates due to multiple ionization are given by

$$\Gamma_{K\alpha} = \Gamma_{K\alpha}^0 \left[ \frac{n_{2p}}{6} \right], \quad (\text{A3a})$$

$$\Gamma_{K\beta} = \Gamma_{K\beta}^0 \left[ \frac{n_{3p}}{6} \right], \quad (\text{A3b})$$

$$\Gamma_A = \Gamma_{KLL}^0 \left[ \frac{n_{2p} + 2}{8} \right] \left[ \frac{n_{2p} + 1}{7} \right] + \Gamma_{KLM}^0 \left[ \frac{n_{2p} + 2}{8} \right] \left[ \frac{n_{3p} + 2}{8} \right] + \dots, \quad (\text{A3c})$$

where  $n_{2p}$  is the number of  $2p$  electrons and  $n_{3p}$  is the number of  $3p$  electrons. It is assumed that only  $s$  and  $p$  electrons participate in the Auger transitions. The expression for  $\Gamma_A$  actually contains several more terms corresponding to transitions of the type  $KMM$ ,  $KMN$ , etc. However, the calculations of Kostroun *et al.*<sup>27</sup> and McGuire<sup>28</sup> show that the first two terms in Eq. (A3c) account for more than 95% of all Auger transitions with the  $KLL$  transitions alone accounting for  $\sim 75\%$  of all transitions. Then, from (A1)

$$\omega_K = \frac{\Gamma_{K\alpha}^0 \left[ \frac{n_{2p}}{6} \right] + \Gamma_{K\beta}^0 \left[ \frac{n_{3p}}{6} \right]}{\Gamma_{K\alpha}^0 \left[ \frac{n_{2p}}{6} \right] + \Gamma_{K\beta}^0 \left[ \frac{n_{3p}}{6} \right] + \Gamma_{KLL}^0 \left[ \frac{n_{2p}+2}{8} \right] \left[ \frac{n_{2p}+1}{7} \right] + \Gamma_{KLM}^0 \left[ \frac{n_{2p}+2}{8} \right] \left[ \frac{n_{3p}+2}{8} \right]} \quad (\text{A4})$$

Rearranging and using Eq. (A2) we get

$$\omega_K = \omega_K^0 \left[ \omega_K^0 + (1 - \omega_K^0) \frac{\left[ 1 + \frac{\Gamma_{K\beta}^0}{\Gamma_{K\alpha}^0} \right] B}{1 + \frac{\Gamma_{K\beta}^0}{\Gamma_{K\alpha}^0} A} \right]^{-1}, \quad (\text{A5a})$$

where

$$A = \frac{n_{3p}}{n_{2p}} \quad (\text{A5b})$$

and

$$B = \frac{6}{n_{2p}} \left[ \frac{\Gamma_{KLL}^0}{\Gamma_A^0} \left[ \frac{n_{2p}+2}{8} \right] \left[ \frac{n_{2p}+1}{7} \right] + \frac{\Gamma_{KLM}^0}{\Gamma_A^0} \left[ \frac{n_{2p}+2}{8} \right] \left[ \frac{n_{3p}+2}{8} \right] \right]. \quad (\text{A5c})$$

It is seen that  $A$  and  $B$  contain all of the dependence on the number of  $2p$  and  $3p$  electrons present at x-ray emission. Putting  $A$  and  $B$  in terms of numbers of vacancies  $V_{2p} = 6 - n_{2p}$  and  $V_{3p} = 6 - n_{3p}$  we get

$$A = \frac{1 - \frac{V_{3p}}{6}}{1 - \frac{V_{2p}}{6}}, \quad (\text{A6a})$$

$$B = \frac{1}{1 - \frac{V_{2p}}{6}} \left[ \frac{\Gamma_{KLL}^0}{\Gamma_A^0} \left[ 1 - \frac{V_{2p}}{8} \right] \left[ 1 - \frac{V_{2p}}{7} \right] + \frac{\Gamma_{KLM}^0}{\Gamma_A^0} \left[ 1 - \frac{V_{2p}}{8} \right] \left[ 1 - \frac{V_{3p}}{8} \right] \right]. \quad (\text{A6b})$$

Then, using Eqs. (A5a), (A6a), and (A6b), we can calculate  $\omega_K$  for multiple  $2p$  and  $3p$  vacancies. The results are given in Table IV. The values of  $\omega_K$  obtained from Eq. (A5a) show almost no beam-energy dependence ( $< 8\%$  in all cases) and so the average value of  $\omega_K$  is used for each target.

It should be noted that Eq. (A5a) for  $\omega_K$  differs significantly from the expression for  $\omega_K$  used by Greenberg *et al.*<sup>29</sup> These authors used an expression for  $\omega_K$  which *only* allowed for  $L$ -shell vacancies. Furthermore, the x-ray transitions were assumed to scale as  $n_L/8$  even though only the  $2p$  electrons contribute to  $K\alpha$  transitions. Hence, Eq. (A5a) should provide a better estimate for  $\omega_K$  in the presence of multiple  $2p$  and  $3p$  vacancies than Eq. (17) in Ref. 29.

\*Present address.

†Present address: Indiana University Cyclotron Facility, Bloomington, IN.

<sup>1</sup>F. Hopkins, Phys. Rev. Lett. **35**, 270 (1975).

<sup>2</sup>T. J. Gray, P. Richard, K. A. Jamison, and J. M. Hall, Phys. Rev. A **14**, 1333 (1976).

<sup>3</sup>H. D. Betz, F. Bell, H. Panke, G. Kalkoffen, M. Welz, and D. Evers, Phys. Rev. Lett. **33**, 807 (1974).

<sup>4</sup>K. O. Groeneveld, B. Kolb, J. Schader, and K. D. Sevier, Z. Phys. A **277**, 13 (1976).

<sup>5</sup>R. K. Gardner, T. J. Gray, P. Richard, C. Schmiedekamp, K. A. Jamison, and J. M. Hall, Phys. Rev. A **15**, 2202 (1977).

<sup>6</sup>F. D. McDaniel, J. L. Duggan, G. Basbas, P. D. Miller, and G. Lapicki, Phys. Rev. A **16**, 1375 (1977).

<sup>7</sup>A. Schmiedekamp, T. J. Gray, B. L. Doyle, and U. Schiebel, Phys. Rev. A **19**, 2167 (1979).

<sup>8</sup>J. A. Tanis, W. W. Jacobs, and S. M. Shafroth, Phys. Rev. A **22**, 483 (1980).

<sup>9</sup>G. Lapicki and F. D. McDaniel, Phys. Rev. A **22**, 1896 (1980). Electron-capture calculations in the present work account also

for the energy-loss effect as does the ECPSSR theory of Ref. 10 for direct ionization.

<sup>10</sup>W. Brandt and G. Lapicki, Phys. Rev. A **23**, 1717 (1981).

<sup>11</sup>R. Rice, G. Basbas, and F. D. McDaniel, At. Data Nucl. Data Tables **20**, 503 (1977).

<sup>12</sup>V. S. Nikolaev, Zh. Eksp. Teor. Fiz. **51**, 1263 (1966) [Sov. Phys.—JETP **24**, 847 (1967)]. The OBK formulas of this reference were obtained using screened hydrogenic wave functions and observed binding energies. These formulas are used in our work without any empirical scaling factors.

<sup>13</sup>E. Storm and H. I. Israel, Nucl. Data Tables A **7**, 565 (1970).

<sup>14</sup>J. H. Scofield, Phys. Rev. A **9**, 1041 (1974).

<sup>15</sup>F. Herman and S. Skillman, *Atomic Structure Calculations* (Prentice-Hall, Englewood Cliffs, 1963).

<sup>16</sup>F. P. Larkins, J. Phys. B **4**, L29 (1971).

<sup>17</sup>J. Hall, P. Richard, T. J. Gray, J. Newcomb, P. Pepmiller, C. D. Lin, K. Jones, B. Johnson, and D. Gregory, Phys. Rev. A **28**, 99 (1983).

<sup>18</sup>Although T. J. Gray, in *Atomic Physics: Accelerators*, Vol. 17 of *Methods of Experimental Physics*, edited by P. Richard



- (Academic, New York, 1980), p. 193, states that with Ref. 9 the need for a scaling factor is eliminated, he and his collaborators continue (see Ref. 17) to use such a factor.
- <sup>19</sup>G. Basbas, W. Brandt, and R. Laubert, *Phys. Rev. A* **17**, 1655 (1978).
- <sup>20</sup>G. Lapicki, *IEEE Trans. Nucl. Sci.* **28**, 1066 (1981).
- <sup>21</sup>T. Gray, P. Richard, G. Gealy, and J. Newcomb, *Phys. Rev. A* **19**, 1424 (1979); R. K. Gardner, T. J. Gray, P. Richard, C. Schmiedekamp, K. A. Jamison, and J. M. Hall, *ibid.* **19**, 1896 (1979); T. J. Gray, C. L. Cocke, and E. Justiniano, *ibid.* **22**, 849 (1980).
- <sup>22</sup>D. H. Madison and E. Merzbacher, in *Atomic Inner-Shell Processes*, edited by B. Crasemann (Academic, New York, 1975), Vol. 1, pp. 1–72.
- <sup>23</sup>E. Merzbacher (private communication).
- <sup>24</sup>G. Lapicki and W. Lichten, *Bull. Am. Phys. Soc.* **29**, 783 (1984).
- <sup>25</sup>J. S. Briggs, *J. Phys. B* **8**, L485 (1975).
- <sup>26</sup>M. O. Krause, *J. Phys. Chem. Ref. Data* **8**, 307 (1979).
- <sup>27</sup>V. O. Kostroun, M. H. Chen, and B. Crasemann, *Phys. Rev. A* **3**, 533 (1971).
- <sup>28</sup>E. J. McGuire, *Phys. Rev. A* **2**, 273 (1970).
- <sup>29</sup>J. S. Greenberg, P. Vincent, and W. Lichten, *Phys. Rev. A* **16**, 964 (1977).